Electron Transfer Reactions in the Excited Singlet States of Dimethyl Substituted Phenol−2-Nitrofluorene Systems: Evidence for the Marcus Inverted Region and Concurrent Occurrence of Energy Transfer Processes

S. Sinha, R. De, and T. Ganguly*

Department of Spectroscopy, Indian Association for the Cultivation of Science, Jadavpur, Calcutta-700 032, India

Received: October 30, 1996; In Final Form: January 17, 1997[⊗]

Studies were made on the nature of photoinduced electron transfer (ET) reactions within the electron donor (D) (3,5-dimethylphenol, 35DMP; 2,6-dimethylphenol, 26DMP; 3,5-dimethylanisole, 35DMA; 2,5-dimethylanisole, 25DMA) and acceptor (A) 2-nitrofluorene (2NF) in both highly polar acetonitrile (ACN) and nonpolar cyclohexane (CH) solvents at 296 K by electronic absorption, steady state, and time-resolved, in the nanosecond time domain, spectroscopic methods. No ground state charge transfer (CT) complex was found for the present D−A pairs. Large fluorescence quenching rates ($\sim 10^{12}$ dm^3 mol^{-1} s^{-1}) were observed in both CH and ACN solvents. Evidence for concurrent occurrence of Förster's type singlet−singlet energy transfer process along with ET was found. No static quenching was observed. Radiative energy transfer was found to play an insignificant role within the present D−A systems. Occurrence of highly exothermic outer-sphere type ET reaction within the Marcus inverted region was inferred. In nonpolar CH a contact exciplex of CT nature was observed, whereas in the highly polar ACN environment the anionic radical of the sterically hindered phenol 2,6-DMP was found as final product. At 77 K occurrences of both Förster's type singlet−singlet and Dexter's type triplet−triplet energy transfer processes were inferred within the present D−A systems from steady state and time-resolved spectroscopic studies.

1. Introduction

Photoinduced electron transfer (ET) reactions are involved as the key steps in photosynthesis and metabolism and in many simple chemical reactions. ET reactions from an excited chromophore (donor) to a molecular acceptor are very important processes, as these events provide a basis for the conversion of light into transiently stored redox energy at the moleculer level.[1,2] Intramoleculer or intermolecular ET reactions have been studied intensively in different D−A (donor−acceptor) systems embedded in a medium such as nonpolar and polar solvents, glass, and proteins.[3−12] Photoinduced intramolecular ET within donor and acceptor molecules linked together by spacers of either flexible[8] or semirigid/rigid types[13,14] is a very interesting subject in the chemistry of photoconductivity[8] and of artificial photosynthesis.[15−20]

Studies on photoinduced ET reactions at 296 K are generally performed in highly polar solvents such as acetonitrile (ACN), where formations of solvent-separated radical ions are genarally facilitated. In a photoinduced ET event where either the donor or acceptor part is in the electronic excited singlet (S_1) state and the other part is in the ground state, primary intermediates might be geminate (or contact) ion pairs (GIP or CIP) or solvent-separated ion pairs (SSIP). The possibility of formation of the former species is rather high in nonpolar environment, whereas the latter one is formed in the highly polar solvent. Emissions could be observed from the GIP (or CIP) but not from the SSIP species because the electronic coupling is much higher in the case of CIP compared to SSIP.[21−23] Earlier workers[23,24] reported that in the cases of some D−A species the back ET reactions occur in the Marcus inverted region (mir). Very few authors located the mir in the forward ET reactions. Rehm and Weller[25] proposed a correlation and demonstrated that even in the highly exothermic region, contrary to the prediction made by Marcus, no inverted region was observed, but instead the fluorescence quenching rate constant (k_q) was found to retain its value equivalent to the diffusion-limited rate throughout this region. Recently, Tachiya[26] gave a new explanation for the lack of the inverted region in forward ET reactions. However Miller et al.[27] demonstrated a decrease of ET rate in the highly exothermic region in the case of intramolecular ET reactions. Ganguly et al.[8] showed from picosecond laser flash photolysis studies the occurrence of photoinduced ET reactions in the inverted region in the cases of several alkylcarbazole−polynitrofluorene and polynitrofluorenone bichromophoric systems and the corresponding oligomers where these bichromophores are present as pendant groups. Recently, Ganguly et al.[28] showed that even in some intermolecular ET cases that are found to be of highly exothermic type the Marcus inverted regions was observed. Testing of inverted regions in the cases of highly exothermic ET reactions has nowadays become a usual practice.[8,28−30]

In the present investigation an attempt was made to examine carefully the nature of photoinduced ET reactions within some disubstituted phenols as donors, 35DMP, 26DMP, 35DMA, and 25DMA, and the well-known acceptor 2NF in polar ACN as well as nonpolar cyclohexane (CH) solvents at 296 K with the help of steady state and time resolved fluorescence techniques. In the framework of Marcus and Rehm−Weller theories and from the observations of large spectral overlapping of donor emission and acceptor absorption another attempt was made to reveal the possible mechanisms of the concurrent processes (if any), e.g., excitational energy transfer and ET, in both nonpolar CH and polar ACN solvents. The rate constants associated with these two basic quenching reactions were evaluated to estimate the relative contributions of these two processes in the quenching phenomena of the electron donors in the presence of the acceptor 2NF.

* To whom all correspondences should be addressed.
[⊗] Abstract published in *Advance ACS Abstracts,* March 1, 1997.

S1089-5639(96)03391-9 CCC: $14.00

TABLE 1: Redox Potentials and Gibbs Free Energies ($\Delta G°$) for the Present D−A Pairs in ACN Fluid Solution at 296 K

donor[a]	acceptor[a]	$E_{1/2}^{OX}(D/D^+)/V$	$E_{1/2}^{RED}(A^-/A)/V$	$E_{0,0}^*/eV$[b]	$\Delta G°$/eV
35DMP*	2NF	1.26	−1.17	4.43	−2.00
35DMP	2NF*	1.26	−1.17	3.75	−1.32
35DMP	2NF	1.26	−1.17		+2.43
26DMP*	2NF	1.53	−1.17	4.43	−1.73
26DMP	2NF*	1.53	−1.17	3.75	−1.05
26DMP	2NF	1.53	−1.17		+2.71
35DMA*	2NF	0.97	−1.17	4.43	−2.29
35DMA	2NF*	0.97	−1.17	3.75	−1.61
35DMA	2NF	0.97	−1.17		+2.15
25DMA*	2NF	1.58	−1.17	4.43	−1.68
25DMA	2NF*	1.58	−1.17	3.75	−1.00
25DMA	2NF	1.58	−1.17		+2.76

[a] * denotes the first excited singlet state (S_1). [b] $E_{0,0}^*$ is the singlet−singlet (0,0) transition energy of the excited chromophore.

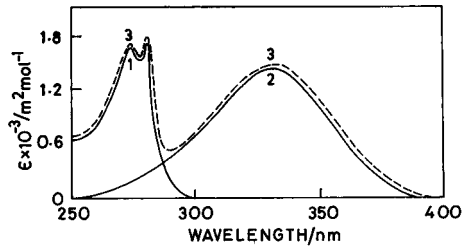

Figure 1. Electronic absorption spectra of 35DMP ($C = 5.6 \times 10^{-5}$ mol dm^{-3}) (curve 1), 2NF ($C = 3.6 \times 10^{-5}$ mol dm^{-3}) (curve 2), and 35DMP ($C = 5.6 \times 10^{-5}$ mol dm^{-3}) in the presence of 2NF ($C = 5.4 \times 10^{-5}$ mol dm^{-3}) (curve 3) in ACN fluid solution ($l = 1$ cm) at 296 K.

The photophysical properties of the present electron donors and the acceptor 2NF were also studied by steady state and time-resolved luminescence techniques at a low temperature of 77 K in an ethanol (EtOH) rigid glassy matrix to observe the effects in their excited singlets and triplets.

2. Experimental Section

2.1. Purification of Chemicals. The samples 35DMP, 26DMP, 35DMA, 25DMA, and 2NF supplied by Aldrich were purified by vacuum sublimation. The solvents ACN, CH, and EtOH (E. Merck) of spectroscopic grade were distilled under vacuum.

2.2. Spectroscopic Apparatus. Steady state electronic absorption and emission spectra of dilute solutions ($\sim 10^{-5}$−10^{-6} mol dm^{-3}) of the samples were recorded at 296 K with the help of a Shimadzu UV−vis 2101PC spectrophotometer and a Hitachi F-4500 fluorescence spectrophotometer, respectively. Fluorescence lifetimes of the samples were measured by using a time-correlated single photon counting (TCSPC) fluorimeter (Model 199, Edinburgh Instruments, U.K.).

All the solutions made for room-temperature measurements were deoxygeneted by purging with a N_2 gas stream for about 30 min. Electrochemical measurements were done (Table 1) by using a PAR 370-4 electrochemistry system.[9] The fluorescence quantum yield (φ_f) of the donor molecules in the absence of the acceptor was determined relative to that of 3-methylindole in CH solvent ($\varphi_f = 0.40 \pm 0.03$).[31]

3. Results and Discussion

3.1. Steady State Electronic Absorption Spectra at 296 K. From Figure 1 it is apparent that the electronic absorption spectra of a present donor in the presence of the acceptor 2NF in polar ACN solvent ($\epsilon_S = 37.5$) result from the superposition of the individual absorption spectra of the components, i.e., donor and acceptor molecules. This indicates that there is no ground state CT interaction between the present donors and 2NF in this solvent.[32] Similar observations were made in nonpolar CH solvent ($\epsilon_S = 2.02$) except that the bands are a little structured. In both the solvents the ^1L_b (S_1) bands of a present donor and 2NF reside at around 280 and 330 nm, respectively.

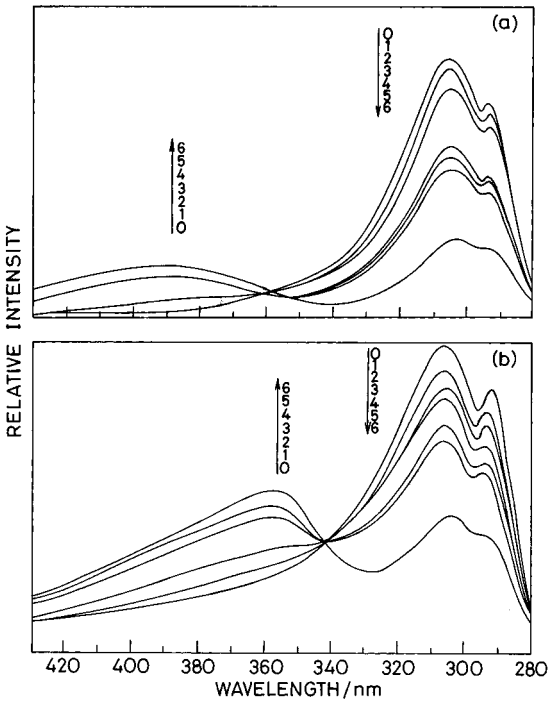

Figure 2. (a) Fluorescence emission spectra of 26DMP in ACN solvent ($C = 1.5 \times 10^{-5}$ mol dm^{-3}) at 296 K ($\lambda_{exc} = 270$ nm) in the presence of 2NF. Concentration of 2NF (mol dm^{-3}): (0) 0; (1) 3.2×10^{-6}; (2) 7.6×10^{-6}; (3) 1.3×10^{-5}; (4) 1.9×10^{-5}; (5) 2.5×10^{-5}; (6) 7.6×10^{-5}. (b) Fluorescence emission spectra of 26DMP in CH solvent ($C = 1.1 \times 10^{-5}$ mol dm^{-3}) at 296 K ($\lambda_{exc} = 270$ nm) in the presence of 2NF. Concentration of 2NF (mol dm^{-3}): (0) 0; (1) 3.2×10^{-6}; (2) 6.3×10^{-6}; (3) 9.5×10^{-6}; (4) 1.3×10^{-5}; (5) 1.6×10^{-5}; (6) 3.2×10^{-5}.

3.2. Steady State and Time-Resolved Spectroscopic Studies at 296 K. The steady state fluorescence intensity of the present donors was found to be reduced gradually with increasing concentration of the quencher 2NF in both ACN (Figure 2a) and CH (Figure 2b) solvents at 296 K. Throughout our experiment, the donor chromophores were selectively excited at the 270 nm position, where the acceptor 2NF has negligible absorbance (Figure 1). This was necessary to avoid the competitive absorption by the acceptor 2NF as well as its filtering effect on the emitted light. Further, 2NF does not exhibit any fluorescence emission at 296 K. The concentration of the quencher 2NF was chosen to be very low ($\sim 10^{-5}$−10^{-6} mol dm^{-3}), which does not affect the electronic absorption spectral pattern (in both intensity and energy position) of the donor molecule. This observation excludes the possibility of any ground state complexation, between the present donor and acceptor molecules, which might be responsible for the observed fluorescence quenching. Figure 2a,b shows that in both ACN and CH solvents the fluorescence emission band of the first singlet excited donor 26DMP peaks at about 305 nm, accompanied by a shoulder at 292 nm which may be assumed as the (0,0) emission band of this donor. With gradual addition of the acceptor 2NF in an ACN fluid solution of 26DMP, relative changes of intensities of the two vibronic bands residing at 292 and 305 nm are observed. Similar observations were noticed for the 35DMP−2NF mixture in ACN as well as CH solvents. In the latter solvent, at a high concentration of 2NF,

TABLE 2: Data on Photoinduced ET (k_{ET}), Förster's Type Energy Transfer (k_{FT}), and the Bimolecular Fluorescence Quenching Rates (k_q) for the Present D−A Pairs at 296 K

systems[a]	τ_0/ns (±0.4)	K_{SV}[b]/ dm^3 mol^{-1}	$k_{q(obs)} \times 10^{-12}$[b]/ dm^3 mol^{-1} s^{-1}	λ[d]/eV	$-\Delta G°$/eV	k_{ET}/s^{-1}	φ_f	R_0/Å	$k_{FT} \times 10^{-11}$/ s^{-1}	$k_{q(calc)} \times 10^{-12}$[e]/ dm^3 mol^{-1} s^{-1}
25DMA*+2NF+ACN	4.9	28 521	5.8	1.52	1.68	8.5×10^{10}	0.14	26	5.4	7.9
		(22 753)[c]	(4.6)[c]							
25DMA*+2NF+CH	3.0	25 885	8.6		0.18					
26DMP*+2NF+ACN	4.2	26 570	6.3	1.15	1.73	5.7×10^{9}	0.09	24	3.4	1.3
		(24 898)[c]	(6.0)[c]							
26DMP*+2NF+CH	5.0	38 566	7.7		0.23					
35DMP*+2NF+ACN	7.1	51 265	7.2	1.13	2.00	1.4×10^{8}	0.13	24	2.5	4.8
		(43 081)[c]	(6.1)[c]							
35DMP*+2NF+CH	5.7	40 591	7.1		0.50		0.08	23	2.0	
35DMA*+2NF+ACN	8.4	15 981	1.9	1.07	2.29	1.2×10^{5}	0.19	27	4.1	7.8
		(13 728)[c]	(1.6)[c]							
35DMA*+2NF+CH	9.8	31 919	3.3		0.79		0.47	32	4.9	

[a] * denotes the first excited singlet state (S_1). [b] Obtained from linear SV plots, using eq 1 (see text). [c] Obtained from linear SV plots, using eq 2 (see text). [d] In calculating λ, $\lambda_V = 0.3$ eV has been chosen (see text). While calculating λ_S, $r_D \approx 3.6$ Å and $r_A \approx 4.4$ Å have been used (see text) and $R = 7$ Å has been assumed (see text). [e] Calculated using eq 15 (see text).

an enhancement in the emission intensity of the (0,0) vibronic band at around 285 nm of the donor 35DMP occurs at the expense of the other band at 293 nm. The same kind of observation was reported earlier by Kalyanasundaram and Thomas[33] in the case of pyrene molecules. Following their argument, it might be proposed that the strong perturbation in the vibronic band intensities is more dependent on the solvent dipole moment than on the bulk solvent dielectric constant.

If the quenching is of dynamic type, a simple Stern−Volmer (SV) relation (eq 1) might be used in evaluating the quenching rate constant (k_q) for the present D−A pairs.[34]

$$f_0/f = 1 + K_{SV}[Q] = 1 + k_q\tau_0[Q] \qquad (1)$$

where f_0 and f are the relative integrated fluorescence emission intensities of the donor without and with the quencher concentration [Q], respectively, K_{SV} is the Stern−Volmer constant, and τ_0 is the fluorescence decay time of the donor in the absence of the quencher. The f_0 and f values were measured from the corrected area under the fluorescence curves. For all present D−A pairs, plots of f_0/f vs [Q](Figure 3) are found to obey the simple SV relation (eq 1), and no upward curvature was noticed even at high concentrations of 2NF, which indicates the absence of static quenching phenomena. Table 2 shows the values of K_{SV} and k_q computed from the linear SV plots (Figure 3) by using eq 1. No major changes were observed in the values of K_{SV} and k_q (Figure 3, Table 2) from lifetime measurements using another form of the SV relation

$$\tau_0/\tau = 1 + K_{SV}[Q] = 1 + k_q\tau_0[Q] \qquad (2)$$

where τ_0 and τ are the fluorescence decay times of the donor without and with the quencher 2NF, respectively. Table 2 shows that there is not much difference in the values of k_q for the present D−A pairs in polar ACN and nonpolar CH solvents. Also the measured values of k_q ($\sim 10^{12}$ dm^3 mol^{-1} s^{-1}) are much higher than the diffusion-controlled limit. The Stern−Volmer data clearly show that no static quenching process occurs. The apparent quenching rate is above the diffusion limit by ~2 orders of magnitude. Therefore, some fast dynamic processes must be operative. Since Stern−Volmer analysis alone does not give information on the mechanism, we discuss possible mechanisms based on literature data and theory. Our aim in this paper is to investigate the individual role of the quenching processes (ET, energy transfer, etc.) involved and to find a correlation between the rate constants of these different processes with the overall fluorescence quenching rate constant k_q.

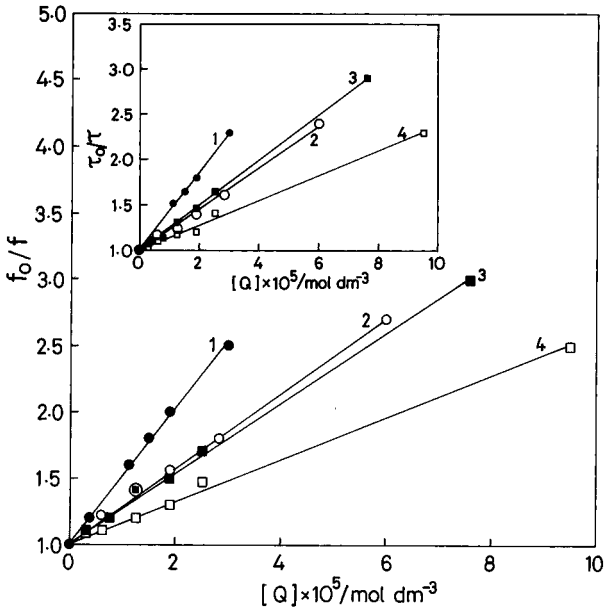

Figure 3. Simple Stern−Volmer (SV) plots by using eq 1 for the present D−A pairs in ACN solvent at 296 K. Inset shows the simple SV plots by using eq 2 for the present D−A pairs in ACN solvent at 296 K (1, 35DMP−2NF; 2, 25DMA−2NF; 3, 26DMP−2NF; 4, 35DMA−2NF).

3.3. Evidence in Support of Exciplex Formation. In the presence of 2NF the fluorescence emission intensity of 26DMP was reduced, accompanied by the appearance of a new broad structureless band on the longer wavelength side at around 355 and 390 nm in CH and ACN solvents, respectively (Figure 2a,b). In CH solvent an isoemissive point was observed. It might be speculated that in nonpolar CH solvent the formation of a contact CT exciplex between 26DMP and 2NF is responsible for the 355 nm band. In polar ACN solvent the exciplex further dissociates into radical ion pairs, giving rise to a new band at 390 nm. We showed by a metallic sodium (Na) experiment that this 390 nm band is due to radical anionic species of the donor 26DMP moiety. O. Brede et al.[35] reported that when some sterically hindered aromatic phenols (ArOH) undergo photoinduced ET reactions with a suitable solvent, radical cations ($ArOH^{\bullet+}$) are formed as intermediates. In polar solvent this cation decays immediately by a dissociation-like deprotonation to form phenoxyl radicals ($ArO^{\bullet}$) and protons as shown below:

$$ArOH^{\bullet+} \rightarrow ArO^{\bullet} + H^{+} \text{ (H atom abstraction)} \qquad (3)$$

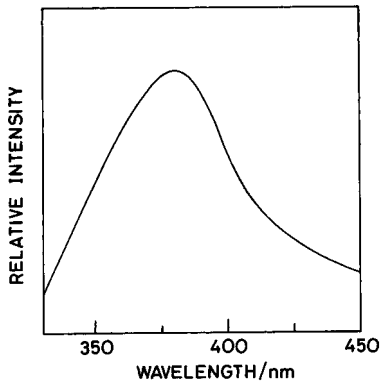

Figure 4. Fluorescence emisssion spectra of 26DMP in dry ACN solvent ($C \approx 10^{-4}$ mol dm^{-3}) at 296 K ($\lambda_{exc} = 270$ nm) in the presence of metallic sodium.

According to O. Brede et al.[35] we could propose the following reaction mechanism for the 2,6-DMP−2NF pair in highly polar ACN environment:

$$2{,}6(CH_3)_2ArOH + 2NF \rightarrow 2{,}6(CH_3)_2ArOH^{\bullet+} + 2NF^- \quad (4)$$

$$2{,}6(CH_3)_2ArOH^{\bullet+} \rightarrow 2{,}6(CH_3)_2ArO^{\bullet} + H^+ \text{ (H atom abstraction)} \quad (5)$$

Here, in eqs 4 and 5 2,6-DMP is written as $2{,}6(CH_3)_2ArOH$ for convenience. Figure 2a demonstrates a clear band at 390 nm of the fluorescence spectra of 2,6-DMP in the presence of 2NF in ACN solvent. To assign unambiguously the true nature of this 390 nm band, the following experiments were performed: (1) In the presence of metallic Na, the fluorescence emission band of 2,6-DMP in dry ACN solvent quenches remarkably with concomitant appearance of a 390 nm band (Figure 4), which gradually disappears in the presence of molecular oxygen. The following reaction should occur between 2,6-DMP and Na:

$$2{,}6(CH_3)_2ArOH + Na \rightarrow 2{,}6(CH_3)_2ArO^- Na^+ + H_2\uparrow \quad (6)$$

Thus, the above observation seemingly indicates that the 390 nm fluorescence band of 2,6-DMP observed in the presence of 2NF in ACN solvent must be due to the formation of phenoxyl radical anion. (2) To corroborate our proposition, excitation spectra of this anion were recorded and were found to be coincident with the absorption spectra of the chemically generated 2,6-DMP$^-$ anion.

However it is rather surprising how the anion is formed from the phenoxyl radical in acidic medium. From all the present experimental findings we possess little doubt about the formation of the 2,6-DMP$^-$ anion. Hence it might happen that due to deprotonation in ACN solvent, the environment may not become acidic to the extent that the formation of anion from the phenoxyl radical (by capturing an electron from the solvent or a neutral donor) could be hindered. However, this is just a matter of speculation. The exact mechanism of formation of the anion from the phenoxyl radical is not very clear at the present stage of investigation. Further investigations with several similar D−A systems are now being carried out to understand this mechanism clearly. This kind of exciplex formation and radical ion pair dissociation were also observed with the 35DMP−2NF pair, but these bands are found to be very weak. The weak behavior might be due to the fact that 35DMP is much less sterically hindered than 26DMP.

3.4. Role of Electron Transfer (ET) in Fluorescence Quenching of the Present Donors in the Presence of the

SCHEME 1

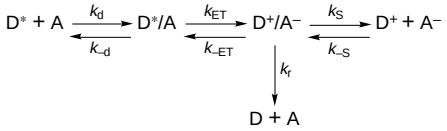

Acceptor 2NF. The Gibbs free energy change ($\Delta G°$) associated with the ET reaction for the present D−A systems was computed by using the well-known Rehm−Weller relation.[25,36]

$$\Delta G° = E_{1/2}^{OX}(D/D^+) - E_{1/2}^{RED}(A^-/A) - E_{0,0}^{*} - e^2/(4\pi\epsilon_0\epsilon_S R) \quad (7)$$

While calculating the values of $\Delta G°$ in highly polar ACN solvent, the Coulomb stabilization term (the fourth term in eq 7) was neglected.[37] From Table 1, it is clear that ET reaction between the present D−A pairs is highly exergonic ($\Delta G° < 0$) and thus energetically probable[37−39] when one of the chromophores, especially the donor chromophore, is excited.

The quenching rate constant for ET could be estimated by employing the mechanistic Scheme 1.[40−42]

In Scheme 1, k_d and k_{-d} are the diffusion-controlled rate constants of second and first-order, respectively, k_{ET} and k_{-ET} are the first-order rate constants for charge separation in the "precursor complex" and charge recombination in the "successor complex", respectively, k_S is the first-order rate constant for the dissociation of the "successor complex", and k_r is the first-order rate constant for reversible electron transfer to ground state reactants. k_{-S} is the rate constant associated with diffusion of charge-separated species to re-form D^+/A^-. However, the possibility of the occurrence of this back process seems to be slim in a highly polar solvent such as ACN, which has a large dielectric constant.

The ET rate constant can be computed from the Arrhenius relation[42]

$$k_{ET} = A \exp(-\Delta G^{\ddagger}/kT) \quad (8)$$

Following Rehm and Weller we set A to be an effective solution-phase collision frequency $A = \nu_n = 1 \times 10^{11}$ s^{-1}.[42] According to Marcus outer-sphere ET theory, the activation energy $\Delta G^{\ddagger}$ is given by[42]

$$\Delta G^{\ddagger} = (\lambda/4)(1 + \Delta G°/\lambda)^2 \quad (9)$$

The reorganization energy λ ($=\lambda_V + \lambda_S$) comprises contributions from both intramolecular bond length changes (λ_V) and solvent reorganization energy (λ_S). λ_S could be computed by using a dielectric continuum model as proposed by Marcus.[3,43]

$$\lambda_S = [e^2/(4\pi\epsilon_0)][1/(2r_D) + 1/(2r_A) - 1/R][1/\epsilon_{OP} - 1/\epsilon_S] \quad (10)$$

For calculating λ_S, the radii (r_D and r_A) have been evaluated from the molecular volume of the neutral molecule.[44] Following Kikuchi,[39] as the ET reactions within the present D−A pairs fall in the highly exothermic region (Table 2), it can be proposed that the ET reactions are of outer-sphere type for which D−A separation distance $R \geq 7$ Å. In calculating λ_S, a fixed value of $R = 7$ Å was chosen for all the D−A pairs. Mataga and others[24] used the same value of R in evaluating λ_s in cases of strong intermolecular ET reactions. While calculating λ, we have chosen a fixed value of $\lambda_V = 0.3$ eV.[8] This value is the characteristic value for aromatic D−A systems.[8] The calculated values of ET rate constant k_{ET} using equation 8 for the present D−A pairs in ACN solvent are shown in Table 2. It is suspected

that ET reactions in the present investigation fall in the Marcus inverted region as $-\Delta G^\circ > \lambda$ (Table 2).

As CH is much less polar than ACN, it is expected that the ET rate constant will decrease in CH solvent as compared to that in ACN. An attempt was made to evaluate k_{ET} for the present D−A pairs in CH solvent by using eq 8. Since we cannot measure redox potentials in CH solvent, we tried to estimate the shift in free energy change (ΔG°) on going from polar ACN to nonpolar CH due to solvation effect. According to Kavarnos et al.,[41] solvation energy is given by

$$\Delta G^\circ(\text{solvation}) = -[e^2/(8\pi\epsilon_0)][1/r_D + 1/r_A][1 - 1/\epsilon_S] \quad (11)$$

Using eq 11, the shift in the value of ΔG° on going from ACN to CH solvent is equal to 1.7 eV. In nonpolar CH solvent, the Coulombic term was fixed, following the Weller assumption,[45] at 0.2 eV for all D−A pairs. So, we can write in the present case

$$\Delta G^\circ(\text{CH}) = \Delta G^\circ(\text{ACN}) + 1.5 \text{ eV} \quad (12)$$

Following Kikuchi,[39] it can be stated that the values of ΔG° in the cases of 3,5-DMP−2NF and 35DMA−2NF pairs in CH solvent fall in the intermediate region (-0.4 eV $> \Delta G^\circ \geq -2.0$ eV)[39] (Table 2), where rapid outer-sphere ET occurs and k_q (due to ET only) should be close to the diffusion-controlled limit ($\sim 6.4 \times 10^9$ dm^3 mol^{-1} s^{-1} in CH solvent) as $-\Delta G^\circ$ is close to λ. For the 3,5-DMP−2NF pair we found k_q (due to ET only) to be equal to $\sim 3.7 \times 10^9$ dm^3 mol^{-1} s^{-1} in CH solvent by using the proposed relation (discussed later) $k_{q(ET)} = k_{ET}k_d/(k_{ET} + k_{-d})$, assuming $R = 7$ Å.[24,39] This observation is in agreement with the theory proposed by Kikuchi.[39]

In the case of other D−A pairs, presently studied, the values of ΔG° in CH solvent fall in the downhill region (0.4 eV $> \Delta G^\circ > -0.4$ eV)[39] (Table 2), where outer-sphere ET is no longer operative. So, in these cases, it was a difficult task to choose the proper value of R while calculating the value of λ_S. So, no definite conclusion could be drawn in the cases of these D−A pairs about the occurrence of ET reaction in CH solvent.

3.5. Energy Transfer as a Possible Mechanism in the Fluorescence Quenching of the Present Donors in the Presence of the Acceptor 2NF. In the present case, the S_1 (^1L_b) level (around 280 nm) of all the donors lies much above the S_1 (^1L_b) level (around 330 nm) of the acceptor 2NF. Also a very good spectral ovarlapping exists between the donor fluorescence emission and acceptor absorption. This allows us to consider two different mechanisms of $S_1^D \rightsquigarrow S_1^A$ energy transfer, radiative (trivial type) and nonradiative. The efficiency of radiative energy transfer (φ_{RT}) was estimated[46] to be $\leq 0.05\%$ for the present D−A pairs (assuming $R = 7$ Å[39]), which is negligible in comparison to nonradiative energy transfer efficiency $T \approx 99.9\%$ (discussed later). From the spectral overlapping, the values of R_0, Förster's critical energy transfer distance for long-range dipole−dipole interactions, were computed[37] for the present D−A pairs (Table 2) and are found to be quite large ($R_0 \approx 25$ Å). This indicates that Dexter's type of energy transfer is not very operative in the present case. The theoretical Förster's energy transfer efficiency, T, was calculated[37] assuming $R = 7$ Å and was found to be more than 99% for the present D−A pairs in ACN as well as CH solvents. This type of $S_1^D \rightsquigarrow S_1^A$ energy transfer generally sensitizes the acceptor fluorescence emission. But as the present acceptor 2NF does not emit any room-temperature fluorescence, spectral manifestation in favor of such energy transfer is lacking. However large values of R_0 (~ 25 Å) and T ($\sim 99.9\%$) predict

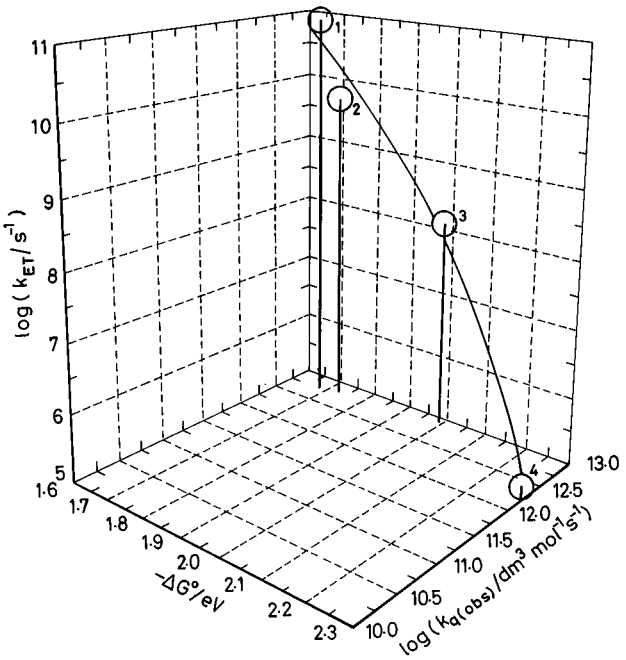

Figure 5. Three-dimensional plot of log k_{ET} (ET rate constant) and log $k_{q(obs)}$ (observed fluorescence quenching rate constant) with Gibbs free energy change ($-\Delta G^\circ$) for the present D−A pairs in ACN solvent at 296 K (1, 25DMA−2NF; 2, 26DMP−2NF; 3, 35DMP−2NF; 4, 35DMA−2NF). k_{ET} values were obtained theoretically by using eq 8 assuming the value of $A = 1 \times 10^{11}$ s^{-1} as proposed by Rehm and Weller.[42] The values of $k_{q(obs)}$ were obtained from the linear SV plots by using eq 1.

SCHEME 2

$$D^* + A \underset{k_{-FT}}{\overset{k_{FT}}{\rightleftharpoons}} D + A^* \xrightarrow{k_N} D + A$$

the concurrent occurrence of long-range singlet−singlet energy transfer along with ET within the present D−A systems.

The simplest representation of Förster's type energy transfer mechanism is shown in Scheme 2, where k_{FT} and k_{-FT} are the forward and back energy transfer rate constants, respectively, and k_N is the rate constant associated with the nonradiative transition of the acceptor from its excited singlet to ground state. The values of Förster's energy transfer rate constant (k_{FT}) were computed by using the relation[37]

$$k_{FT} = (1/\tau_0)(R_0/R)^6 \quad (13)$$

and are shown in Table 2, which indicates that Förster's type energy transfer is playing a dominant role in the fluorescence quenching phenomena in both ACN and CH solvents (assuming $R = 7$ Å[39]) as k_{FT} values ($\sim 10^{11}$ s^{-1}) are much greater than k_{ET} values (Table 2).

3.6. Correlation between Electron Transfer Rate Constant (k_{ET}), Förster's Energy Transfer Rate Constant (k_{FT}), and Fluorescence Quenching Rate Constant (k_q) for the Present D−A Pairs in ACN Solvent. Applying a steady state treatment to the various intermediates in Schemes 1 and 2 leads to[47]

$$k_q = \frac{k_{FT}}{k_{-FT} + k_N} \frac{k_d}{1 + k_{-d}/k_{ET} + k_{-d}k_{-ET}/[(k_S + k_r)k_{ET}]} \quad (14)$$

For exothermic forward ET reaction, we assume $k_{-ET} \ll k_{ET}$. Also k_{-FT} is assumed to be neglegible as k_{FT} is very high. Then eq 14 becomes[48,49]

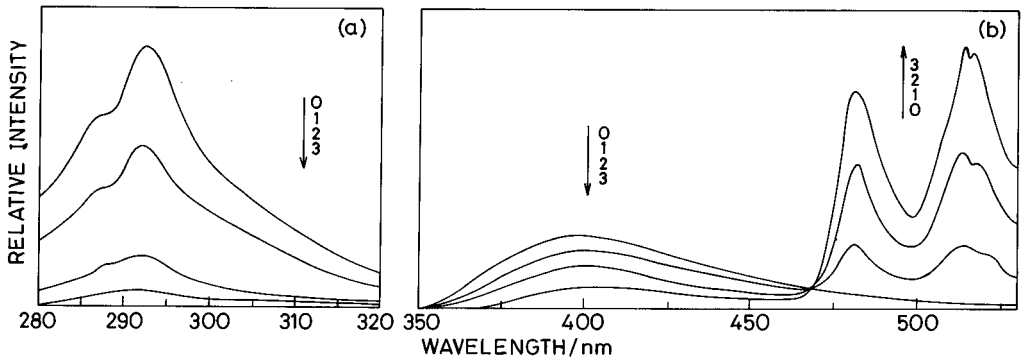

Figure 6. (a) Fluorescence emission spectra of 35DMA ($C = 7.2 \times 10^{-5}$ mol dm^{-3}) in an EtOH rigid glassy matrix at 77 K ($\lambda_{exc} = 270$ nm) in the presence of 2NF. Concentration of 2NF (mol dm^{-3}): (0) 0; (1) 3.6×10^{-4}; (2) 1.5×10^{-3}; (3) 2.9×10^{-3}. (b) Phosphorescence emission spectra of 35DMA ($C = 7.2 \times 10^{-5}$ mol dm^{-3}) in an EtOH rigid glassy matrix at 77 K ($\lambda_{exc} = 270$ nm) in the presence of 2NF. Concentration of 2NF (mol dm^{-3}): (0) 0; (1) 3.6×10^{-4}; (2) 1.5×10^{-3}; (3) 2.9×10^{-3}.

$$k_q = \frac{k_{FT}}{k_N} \frac{k_{ET} k_d}{k_{ET} + k_{-d}} \qquad (15)$$

Here, we set $k_N = 1 \times 10^9$ s^{-1}.

The computed values of fluorescence quenching rate constant $k_{q(calc)}$ (using eq 15) and the observed values of quenching rate constant $k_{q(obs)}$ (using SV relation 1) for the present D−A pairs in ACN solvent are shown in Table 2. An excellent agreement was noticed between the values of $k_{q(calc)}$ and $k_{q(obs)}$ for 25DMA−2NF and 26DMP−2NF systems, for which the values of $\Delta G°$ fall in the intermediate region (-0.4 eV $> \Delta G° \geq -2.0$ eV).[39] For the 35DMP−2NF and 35DMA−2NF systems the values of $\Delta G°$ fall in the highly exothermic region ($\Delta G° \geq -2.0$ eV).[39] To obtain a good agreement between the values of $k_{q(calc)}$ and $k_{q(obs)}$ for these systems, it was found to be necessary to omit k_{-d} in eq 15 while calculating the values of $k_{q(calc)}$. This assumption seems to be quite justified on the grounds that in the highly exothermic region in the present case Förster's energy transfer process dominates over ET reactions, as evidenced from the observed respective rate constant values (Table 2).

From the 3D graph in Figure 5, we could reach two important conclusions: (1) ET reactions in the present investigation fall in the Marcus inverted region where the photoinduced ET rate (k_{ET}) decreases with an increase of exothermicity. (2) There is little variation in the observed fluorescence quenching rate constant ($k_{q(obs)}$) with the driving force ($\Delta G°$), which suggests that ET reactions play a minor role in nonradiative depletion of the excited singlet (S_1) states of the present donors in the presence of the acceptor 2NF in ACN solvent. Thus Figure 5 indicates that the other nonradiative process, $S_1^D \rightsquigarrow S_1^A$ energy transfer, largely dominates over the ET process in quenching of the donor fluorescence. From the estimated rate constant values, we made the same conclusions as discussed above.

3.7. Analysis of Fluorescence and Phosphorescence Spectra of the Present D−A Pairs at 77 K. At 77 K both the fluorescence and broad phosphorescence emission spectra of a present donor, produced due to excitation of S_1 band, in an EtOH rigid glassy matrix were found to quench regularly on increasing the concentration of the acceptor 2NF (Figure 6a,b) with concomitant appearance of the phosphorescence band of 2NF (which extends from 470 up to 520 nm, the (0,0) band being at 480 nm, Figure 6b). It is suspected that a Förster's type energy transfer process (as at 77 K, the values of R_0, measured from the considerable spectral overlapping between donor fluorescence emission and acceptor absorption spectra, and the fluorescence lifetime of the donor remain practically the same) is still responsible, like the situation at ambient temperature, for the fluorescence quenching of the present donors in presence of the acceptor 2NF at 77 K. On the other hand ET reaction, being a thermally activated process, is expected to have less effect on the fluorescence quenching of the donors as compared to that at room temperature.[50,51]

It is observed that the phosphorescence quenching of a present donor occurs in the presence of 2NF with concomitant appearance of a band at longer wavelength (Figure 6b). Monitoring wavelengths located at different positions (480 and 510 nm) of this long-wavelength phosphorescence band, it was found that the lifetime, τ_p, is on the order of 0.2 s, which corresponds to the phosphorescence lifetime of the acceptor 2NF only. Thus both from steady state and time-resolved data it can be inferred that the phosphorescence quenching of the present donors in the presence of 2NF mainly proceeds through triplet−triplet ($T_1^D \rightsquigarrow T_1^A$) energy transfer by an exchange mechanism from the donors to the acceptor 2NF.

4. Concluding Remarks

The possibility of ground state CT complex formation between the present D−A systems in both ACN and CH solvents is ruled out from the observations of steady state electronic absorption spectra at 296 K.

Large fluorescence quenching of all the present donors was found to occur at 296 K in the presence of the acceptor 2NF in ACN as well as CH solvents. Two basic quenching processes, viz., photoinduced ET and Förster's type singlet−singlet energy transfer, seem to be responsible for the observed fluorescence quenching, and the latter process was seen to play a dominant role over the former one. No static quenching phenomena were observed. From the relative studies of the values of nuclear reorganization energy (λ) and Gibbs free energy ($\Delta G°$), the highly exothermic ET reactions between the present D−A pairs in ACN solvent appear to be in the Marcus inverted region ($-\Delta G° > \lambda$). Moreover, observation of a decrement of k_{ET} with an increase of exothermicity corroborates this proposition. In the case of the 26DMP-2NF pair, an exciplex of contact CT nature was found in nonpolar CH solvent at the 355 nm position at 296 K. From a detailed spectral analysis it seemingly indicates that this exciplex dissociates to form an anionic radical of 26DMP in polar ACN solvent as a final product, which emits at around 390 nm, through an ET process, followed by dissociation-like deprotonation. However, the exact mechanism of formation of anionic species is not very clear at the present stage of investigation. This kind of exciplex formation and radical ion pair dissociation was also observed in the case of the 35DMP−2NF pair, but a very weak fluorescence emission band of this species was observed. This weak behavior has

been explained to be due to the fact that 35DMP is less sterically hindered than 26DMP.

At 77 K in an EtOH rigid glassy matrix, occurrences of both singlet−singlet and triplet−triplet energy transfer processes from the excited donors to acceptor were inferred from steady state measurements and time-resolved emission spectroscopic studies as well.

Acknowledgment. We thank Dr. N. Chattopadhyay and Dr. S. C. Bera of Jadavpur University for fluorescence lifetime measurements and the Inorganic Chemistry Department of IACS for performing the electrochemical measurements. T.G. especially thanks his colleague Dr. B. Ranu of the Organic Chemistry Department for very helpful discussions.

References and Notes

(1) (a) Fox, M. A., Chanon, M., *Eds. Photoinduced Electron Transfer;* Elsevier: Amsterdam, 1988. (b) Gratzel, M. *Heterogeneous Photochemical Electron Transfer;* CRC: Boca Raton, FL, 1989.
(2) Castellano, F. N.; Meyer, G. J. *J. Phys. Chem.* **1995,** *99,* 14742.
(3) Marcus, R. A. *J. Chem. Phys.* **1956,** *24,* 966.
(4) Marcus, R. A. *Annu. Rev. Phys. Chem.* **1964,** *15,* 155.
(5) Newton, M. D.; Sutin, N. *Annu. Rev. Phys. Chem.* **1984,** *35,* 437.
(6) Marcus, R. A.; Sutin, N. *Biochim. Biophys. Acta* **1985,** *811,* 265.
(7) Jortner, J., Pullman, B., *Eds. Perspectives in Photosynthesis;* Kluwer: Dordrecht, 1990.
(8) Ganguly, T.; Sharma, D. K.; Gauthier, S.; Gravel, D.; Durocher, G. *J. Phys. Chem.* **1992,** *96,* 3757.
(9) Jana, P.; De, R.; Ganguly, T. *J. Lumin.* **1994,** *59,* 1.
(10) Jortner, J.; Bixon, M. *J. Photochem. Photobiol. A: Chem.* **1994,** *82,* 5. Siddarth, P.; Marcus, R. A. *J. Phys. Chem.* **1993,** *97,* 6111.
(11) Ke, W.; Wu, J. *Spectrochim. Acta, Part A* **1995,** *51,* L25.
(12) De, R.; Jana, P.; Ganguly, T. *Spectrochim. Acta, Part A,* in press.
(13) Kroon, J.; Oevering, H.; Verhoeven, J. W.; Warman, J. M.; Oliver, A. M.; Paddon-Row, M. N. *J. Phys. Chem.* **1993**, *97,* 5065.
(14) Jordon, K. D.; Paddon-Row, M. N. *Chem. Rev.* **1992,** *92,* 395.
(15) Gatzen, G.; Miller, M. G.; Griebenow, K.; Hotzwarth, A. R. *J. Phys. Chem.* **1996,** *100,* 7269.
(16) Rempel, U.; Von Maltzan, B.; Von Borczyskowski, C. *Chem. Phys. Letts.* **1995,** *245,* 253.
(17) Franzen, S.; Goldstein, R. F.; Boxer, S. G. *J. Phys. Chem.* **1993,** *97,* 3040.
(18) Tang, J.; Norris, J. R. *Chem. Phys.* **1993,** *175,* 337.
(19) Pollinger, F.; Heitele, H.; Michel-Beyerle, M. E.; Tercal, M.; Staal, H. A. *Chem. Phys. Lett.* **1993,** *209,* 251.
(20) Van Dijk, S. I.; Wiering, P. G.; Van Staveren, R.; Van Ramesdonk, H. J.; Brouwer, A. M.; Verhoeven, J. W. *Chem. Phys. Letts.* **1993,** *214,* 502.
(21) Gould, I. R.; Farid, S.; Young, R. H. *J. Photochem. Photobiol. A: Chem.* **1992,** *65,* 133.
(22) Gould, I. R.; Young, R. H.; Moody, R. E.; Farid, S. *J. Phys. Chem.* **1991,** *95,* 2068.
(23) Gould, I. R.; Farid, S. *J. Phys. Chem.* **1992,** *96,* 7635.
(24) Mataga, N.; Shioyama, H.; Kanda, Y. *J. Phys. Chem.* **1987,** *91,* 314.
(25) Rehm, D.; Weller, A. *Isr. J. Chem.* **1970,** *8,* 259.
(26) Tachiya, M.; Murata, S. *J. Phys. Chem.* **1992,** *96,* 8441.
(27) Miller, J. R.; Calcaterra, L. T.; Closs, G. L. *J. Am. Chem. Soc.* **1984,** *106,* 3047.
(28) De, R.; Bhattacharyya, S.; Ganguly, T. *Spectrochim. Acta* **1994,** *50A,* 2155.
(29) Gould, I. R.; Ege, D.; Moser, J. E.; Farid, S. *J. Am. Chem. Soc.* **1990,** *112,* 4290.
(30) Warman, J. M.; Smit, K. J.; de Haas, M. P.; Jonker, S. A.; Paddon-Row, M. N.; Oliver, A. N.; Kroon, J.; Oevering, H.; Verhoeven, J. W. *J. Phys. Chem.* **1991**, *95,* 1979; *J. Am. Chem. Soc.* **1990,** *112,* 4868.
(31) Meech, S. R.; Phillips, D. *Chem. Phys.* **1983,** *80,* 317.
(32) Helsen, N.; Viaene, L.; Van der Auweraer, M.; De Schryver, F. C. *J. Phys. Chem.* **1994**, *98,* 1532, and references therein.
(33) Kalyanasundaram, K.; Thomas, J. K. *J. Am. Chem. Soc.* **1977,** *99,* 2039.
(34) Rubio, M. A.; Lissi, E. A. *J. Photochem. Photobiol. A: Chem.* **1993,** *71,* 175.
(35) Brede, O.; Orthner, H.; Zubarr, V.; Hermann, R. *J. Phys. Chem.* **1996,** *100,* 7097.
(36) Rehm, D.; Weller, A. *Ber. Bunsen.-Ges. Phys. Chem.* **1969,** *73,* 834.
(37) Zelent, B.; Messier, P.; Gravel, D.; Gauthier, S.; Durocher, G. *J. Photochem. Photobiol. A: Chem.* **1987,** *40,* 145.
(38) Chibisov, A. K. *Usp. Khim.* **1981,** *50,* 1169; *Prog. React. Kinet.* **1984,** *13,* 1.
(39) Kikuchi, K. *J. Photochem. Photobiol. A: Chem.* **1992,** *65,* 149.
(40) Zeng, H.; Sow, M.; Durocher, G. *J. Lumin.* **1994,** *62,* 1.
(41) Kavarnos, G. J.; Turro, N. J. *Chem. Rev.* **1986,** *86,* 401.
(42) Chen, J. M.; Ho, T. I.; Mou, C. Y. *J. Phys. Chem.* **1990,** *94,* 2889.
(43) Marcus, R. A. *J. Chem. Phys.* **1957,** *26,* 867.
(44) Oevering, H.; Paddon-Row, M. N.; Heppener, M.; Oliver, A. M.; Cotsaris, E.; Verhoeven, J. W.; Hush, N. S. *J. Am. Chem. Soc.* **1987,** *109,* 3258.
(45) Weller, A. *Z. Phys. Chem.* **1982,** *133,* 93.
(46) Mugnier, J.; Pouget, J.; Bourson, J.; Valeur, B. *J. Lumin.* **1985**, *33,* 273.
(47) Rice, S. A. In *Comprehensive Chemical Kinetics;* Bamford, C. A., Tipper, C. F. H., Compton, R. G. Eds.; Elsevier: Amsterdam,1985; p 25.
(48) Marcus, R. A. *Int. J. Chem. Kinet.* **1981**, *13,* 865.
(49) Sutin, N. *Acc. Chem. Res.* **1982**, *15,* 275.
(50) Mikkelsen, K. V.; Ratner, M. A. *Chem. Rev.* **1987**, *87,* 113.
(51) Siemiarczuk, A.; Mcintosh, A. R.; Bolton, J. R.; Connolly, J. S. *J. Am. Chem. Soc.* **1983**, *105,* 7224.
(52) Marsh, D. J.; Lowey, S. *Biochemistry* **1980**, *19,* 774.